Limnol. Oceanogr., 39(5), 1994, 1211–1222

Microautoradiography (with combined liquid scintillation) applied to the study of trace metal uptake by suspended particles: Initial results using ^{63}Ni as a tracer

Abstract—We report the development of a microautoradiographic method for the study of trace metal–particle interactions in natural waters. This technique, in combination with conventional liquid scintillation counting methods, was applied to surface water samples from the Belgian coastal zone and Scheldt estuary. ^{63}Ni was used as the metallic radiotracer. Ni partitioning in our experimental system was shown to be a primarily abiotic process, driven by passive sorption reactions and limited in extent on a 24-h time scale by the slow reaction kinetics of Ni. Small particles (< 1 μm) were important as sorption sites, while large particles exhibited variable and particle-specific scavenging potential.

The cycling of trace metals in the marine environment is a complex process, influenced by many geochemical, physical, and biological parameters. The removal of dissolved metal species from the water column by particles (i.e. scavenging) is a fundamental step in the cycle, leading to the deposition of trace elements in the sediment. The drive to understand particle-mediated removal processes has, in the last decade, led to intensive research on the nature of particle–metal interactions in the water column.

Laboratory studies of metal uptake have been instrumental in elucidating the kinetic aspects of trace metal sorption (e.g. Nyffeler et al. 1984; Jannasch et al. 1988). Sorption here is taken to include all processes responsible for the transfer of metals from the dissolved to the solid phase. In the basic methodology of such experiments, the uptake of a radiotracer onto a well-defined solid phase or a natural collection of particulates in aqueous suspension is monitored over time by periodically filtering solids out and radiochemically counting the filters.

This technique has been modified for field application by several workers (Wollast and Loijens 1991; Moffett 1990) to study the biological and chemical processes behind the kinetics of metal uptake in natural systems. Wollast and Loijens (1991) have combined the basic radiotracer experiment with different incubation conditions (light, dark, azide inhibition) and concurrent measurement of ^{14}C primary productivity to determine the role of active phytoplankton assimilation in scavenging. Moffett (1990) has also used varied incubation conditions along with ascorbate treatments to identify the significance of microbial Mn oxidation in the scavenging of metals such as Ce.

A natural extension of such process-oriented work in complex marine environments would be to identify the different scavenging mechanisms at work in a heterogeneous particle matrix, along with their relative significance. To achieve this level of understanding in a radiotracer experiment, it is necessary to identify in some detail which components of a given particle assemblage are associated with the tracer. In the work presented here, we demonstrate the use of a microautoradiographic technique to obtain such information.

Grain-density microautoradiography uses a photographic film coating over microscopically mounted radiolabeled objects to visualize the location of a radiotracer on particles at the level of light or electron microscopy. Precedent for the use of microautoradiography to study marine particles comes from the field of marine ecology, in which microautoradiography with ^{14}C- and ^{3}H-labeled substrates has been used to study primary productivity (Davenport and Maguire 1984; Knoechel and Kalff 1976) and bacterial metabolism (Douglas et al. 1987; Ward 1984). The technique detailed here is based largely on the work of Meyer-Reil

Acknowledgments

This research was funded by a Fulbright-Hays Student Grant for study in Belgium.

Gilles Billen and the members of his research group are gratefully acknowledged for their sampling assistance and data on suspended matter at station 330. Thanks to L. Chou, J. Moffett, M. Bacon, K. Buesseler, E. Sholkovitz, D. Caron, F. M. M. Morel, and two anonymous reviewers for helpful comments.

(1978) and Tabor and Neihof (1982). The choice of tracer was constrained by the necessity of using a metallic radioisotope with a mode of decay appropriate to autoradiographic recording. Although ^{63}Ni has not been as widely applied to autoradiography as some other metallic radioisotopes like ^{65}Zn (Fowler et al. 1970) or ^{55}Fe (Hutchins et al. 1993), the low-energy (0.067 Mev) soft-beta emissions of the isotope make it ideal for high-resolution microscopic studies using very thin emulsion coatings. In addition, the vertical distribution of Ni in the oceanic water column (Bruland 1980) indicates that Ni is involved in some scavenging process.

The data set presented here is limited, and we therefore regard our results as provisional. We present quantitative data on ^{63}Ni partitioning, obtained by established methods of liquid scintillation counting, together with qualitative data obtained by microautoradiography. Our intention is to explain the details of the autoradiographic method and to demonstrate its feasibility and potential value as a tool for studying trace metal–particle interactions in combination with more conventional methods.

Samples for this work were obtained as part of a larger program (of G. Billen) to monitor the spring bloom of *Phaeocystis pouchetii* in the southern bight of the North Sea. Samples were taken from the surface water at station 330, located in the Belgian coastal zone, 10 km off Ostend (51°26′05″N, 2°49′08″E). This site has been described previously by Lancelot and Mathot (1987). Additional samples for our experiments were taken from the Scheldt estuary, at a point roughly 80 km up the estuary, salinity of ~5. It was felt that by sampling several times over the course of a bloom, and in both ocean and estuarine locations, the technique could be applied to a wide variety of particulate assemblages.

Samples were collected in acid-cleaned plastic containers and stored in darkness at 4°C for transport back to the laboratory (<4 h). Upon arrival at the laboratory, subsamples were dispensed into acid-cleaned 200-ml polycarbonate Co-Star culture bottles for liquid scintillation experiments, or 20-ml polycarbonate test tubes for autoradiography experiments. Subsample inhomogeneity was avoided by thoroughly mixing the original sample before dispensing each subsample. In addition to adding ^{63}Ni to samples for both liquid scintillation counting and autoradiography, some separate samples were spiked with ^{14}C for liquid scintillation counting in order to determine levels of primary productivity.

Samples were spiked with a solution of ^{63}Ni as Ni(II)chloride in dilute (<0.01 M) HCl or a $H^{14}CO_3$ solution (Amersham Radiochemicals). ^{14}C was added to samples at a level of 0.22 MBq per 100 ml. For liquid scintillation analysis of ^{63}Ni uptake, samples were spiked with ~30 nM of the Ni(II)chloride solution, resulting in an activity of about 0.085 MBq per 100 ml. Samples for autoradiographic analysis were spiked to about twice that level. Although ambient Ni concentrations in our samples were not determined, it should be noted that concentrations of dissolved Ni off the Belgian coastal zone have recently been determined at 6–10 nM during this season (Zhang unpubl. data), while those in the upper Scheldt are ~150 nM (Wollast unpubl. data). Although it would have been desirable to add the Ni in tracer amounts, the fact that the ^{63}Ni was not carrier-free precluded this possibility for the coastal samples. It was determined that adding 30–60 nM Ni reduced the ^{14}C uptake in our coastal samples by ~20%, thus indicating some reduction in algal growth. Due to these conditions, the results of this study are not necessarily reflective of processes affecting Ni uptake in natural marine systems.

Incubations were performed on a shaker at 8°C for periods of not longer than 24 h. Various incubation conditions included constant fluorescent light, constant darkness, or bioinhibition with 1.2% sodium azide. (This concentration of azide inhibited ^{14}C uptake in our marine samples by ~90%, but its effect on bacterial metabolism was not determined.) Nonlabeled incubations for autoradiographic controls were performed at the same time under identical conditions.

For liquid scintillation samples, unfiltered 1-ml subsamples were taken immediately after tracer addition and again immediately before sample filtration. Both subsamples were counted to ensure that no significant amount of tracer was lost to the walls of the polycarbonate bottles. At time intervals ranging from 10 min to 24 h, 50–200 ml of sample (depending on filter pore size and particle density)

Table 1. Effect of rinsing on ^{63}Ni retention by particles (station 330, 5 June, 24-h incubation, 0.2-μm filter).

Type of incubation	^{63}Ni uptake for various types of seawater rinses (%)		
	Ni-spiked seawater (30 nM)	Natural seawater	EDTA seawater (10^{-4} M)
Light	0.57	0.51	0.48
Azide	0.49	0.40	0.43

were filtered at low pressure (<250 mm of Hg). ^{14}C samples were passed through Whatman GF/F 0.7 μm filters. Filters for ^{14}C analysis were fumed over HCl to remove inorganic ^{14}C, and filtrate subsamples for analysis were mixed with 50% vol/vol 1 N NaOH to prevent ^{14}C loss. ^{63}Ni samples were passed through Sartorious 47-mm 0.2- and 0.45-μm cellulose acetate filters. All ^{63}Ni samples were rinsed after filtration with 10 ml of 0.2-μm-filtered seawater (or Milli-Q water for the Scheldt sample) spiked with 30 nM of nonradioactive Ni(II) chloride. Rinse water was spiked to minimize the Ni concentration gradient between samples and rinse. This method caused slightly less adsorbed ^{63}Ni loss than rinsing with plain filtered seawater (Table 1).

All liquid scintillation samples were analyzed on a Packard Tri-Carb 3255 liquid scintillation counter, with an external standard solution of ^{14}C hexadecane to determine counting efficiency. Quench potentials of liquid and solid samples were equalized by adding 1 ml of Milli-Q water to the filter plus 10 ml of Beckman Ready Safe liquid scintillator. ^{63}Ni uptake at each time point was calculated as Filter/(Filter + Filtrate) (in %). By calculating uptake in this way, wall-adsorption effects are accounted for, and the change in the relative percent of ^{63}Ni over time on the solid phase is clearly shown. ^{14}C uptake was calculated as Filter/Total (in %), using the initial unfiltered subsamples as the value of Total.

Following 24 h of incubation, all autoradiographic samples were preserved by adding 1% ethanol. Subsamples (1–5 ml, depending on particle density) were passed at low pressure (<250 mm of Hg, to minimize cell damage) through 25-mm 0.2-μm Nuclepore polycarbonate filters within 3 h of preservation. Filters were then rinsed with 10 ml of 0.2-μm filtered seawater (Milli-Q water for Scheldt samples) spiked with 60 nM of nonradioactive Ni(II) chloride.

Immediately following filtration, filters were cut into quarters and the quarters placed sample side down on an acid-cleaned, gelatin-coated slide (gelatin solution—5% gelatin, 0.05% chrome alum, both Merck). Prior to applying filters, coated slides were steamed over a beaker of boiling Milli-Q water for several seconds to soften the gelatin. After thorough drying, slides with mounted samples were dipped into 1% glycerol for several seconds and allowed to dry again before filters were peeled away. This method (adapted from Tabor and Neihof 1982) has been found to give virtually complete sample retention on the slide.

Samples for epifluorescent viewing were mounted in identical fashion, but on subbed coverslips mounted on slides so that the finished preparations could be turned over and viewed with the sample in between the emulsion and the microscope lens. Nonradioactive controls for positive and negative chemography (chemical effects on emulsion which can cause spurious grain formation or grain removal) were preserved, filtered, and mounted in the same fashion as labeled samples.

In a darkroom under low safelighting at +75% relative humidity, mounted samples were dipped in Amersham LM-1 autoradiographic emulsion (diluted 1 part emulsion to 2 parts Milli-Q water) held at 38°C. Immediately after dipping (without draining), slides were placed on a chilled metal plate to gel the emulsion. The plate was sealed in a light-tight box, and slides were allowed to dry for 3 h. Silica gel was then placed in the box and the slides left overnight. All subsequent steps were carried out in complete darkness to reduce background.

Prior to insertion into exposure boxes, all slides were dipped into Beckman Ready Safe liquid scintillator. This procedure (adapted from Durie and Salmon 1975) reduced exposure time by amplifying the number of silver grains produced for each decay event. Several control slides in each batch were exposed to light before exposure to act as controls against latent image fading and negative chemography. Each batch also included several non-light-exposed, nonradioactive control slides for false positive results.

Optimum exposure conditions for slides were

19 d at −12°C in the presence of silica gel. At the end of the exposure period, slides were developed in a dilute amidol developer (250 ml of Milli-Q water, 1.125 g of anhydrous sodium sulfite, 0.2812 g of Amidol, 0.5 ml of 10% KBr solution, all chemicals Merck), dipped in 0.5% glacial acetic acid solution for 30 s, and then fixed in 30% sodium thiosulfate solution for 8 min. After extensive rinsing in distilled and Milli-Q water, half the slides in each sample and control set were stained with methyl-green pyronin stain (Aldrich) for 20 min and destained in 70% ethanol for 1 min (Rogers 1973). The remaining half of each sample and control set was stained in 8.6 M 4′,6-diamidino-2-phenylindole (DAPI) (Boehringer-Manneheim) for 1 h and rinsed with Milli-Q water (Porter and Feig 1980). All development and staining procedures were carried out at room temperature.

Autoradiograms stained with methyl-green pyronin were viewed and photographed on a Zeiss photo microscope under oil immersion with transmitted light. Kodak TMax 100 black-and-white 35-mm film was used for photos. DAPI-stained autoradiograms, of which no photographs were taken, were examined under alternate transmitted and epifluorescent lighting on a Leitz fluorescence microscopy system.

Autoradiographic analysis was strictly qualitative, the intention being to determine general trends in Ni adsorption over the various particulate fractions (i.e. phytoplankton, bacteria, detritus, inorganics) in each sample. In these categorizations, detritus is taken to refer to biogenic material not present as discrete cells, while inorganics (most likely metal oxides) were identified mainly by their crystalline appearance and lack of staining under the microscope.

Methyl-green pyronin-stained autoradiograms were used to determine labeling of particles larger than developed silver grains (grains ~0.2 μm in diameter). Background grain counts, as determined by nonlabeled control slides, were normally on the order of 5–7 grains per oil immersion field (125× magnification). Such low backgrounds enabled detection of labeling at very low levels, the limit being about 3–5 grains localized over 5 μm^2 of particulate surface area. Very large dense detrital aggregations (>100 μm in diameter) were omitted from this analysis due to chemographic effects observed on controls (desensitization of emulsion).

Labeling of small (<1 μm) cells was estimated by viewing DAPI-stained autoradiograms under alternating fluorescent and transmitted light in order to correlate the location of grains and fluorescent cells. Those grains not associated with fluorescent cells on DAPI-stained slides were considered as labeled small inorganic or detrital particles. Because background counts as determined by DAPI-stained control slides were so low (again 5–7 grains per field), background grains were neglected in these rough estimations of Ni-uptake patterns.

Determinations of suspended matter in the station 330 samples were carried out in the laboratory of Gilles Billen using 0.7-μm Whatman GF/F filters. (*See* Lancelot and Mathot 1987 for methods.)

Detailed studies of ^{63}Ni uptake kinetics were carried out on two representative samples, the station 330 sample taken on 22 May and the Scheldt estuary sample taken on 25 May. In comparing the results for each sample (Fig. 1), it is necessary to keep in mind the quality of the two environments considered. In addition to the great difference in salinity between the coastal North Sea (station 330) and the Scheldt estuary, there was also a vast disparity in the particulate load of the samples (58.2 mg $liter^{-1}$ in the Scheldt, 17.33 μg $liter^{-1}$ for station 330, 22 May).

On the basis of these particle concentrations and the data in Fig. 1, the log of the experimental partition coefficient (log K_d) at 24 h is ~3.1 for the Scheldt and 3.8 for station 330. This result is somewhat contradictory to expectations based purely on salinity considerations, where one would predict higher metal partitioning in lower salinity waters. One possible explanation for the data is that the lower partitioning in the Scheldt sample is due to the "particle concentration effect" documented by Honeyman and Santschi (1988), in which K_d has been observed to decrease with increasing particle concentration.

It is apparent that the basic shapes of the adsorption curves in Fig. 1 are similar, despite the aforementioned differences in salinity and particle concentration. There was a rapid initial uptake in both samples, occurring in <10

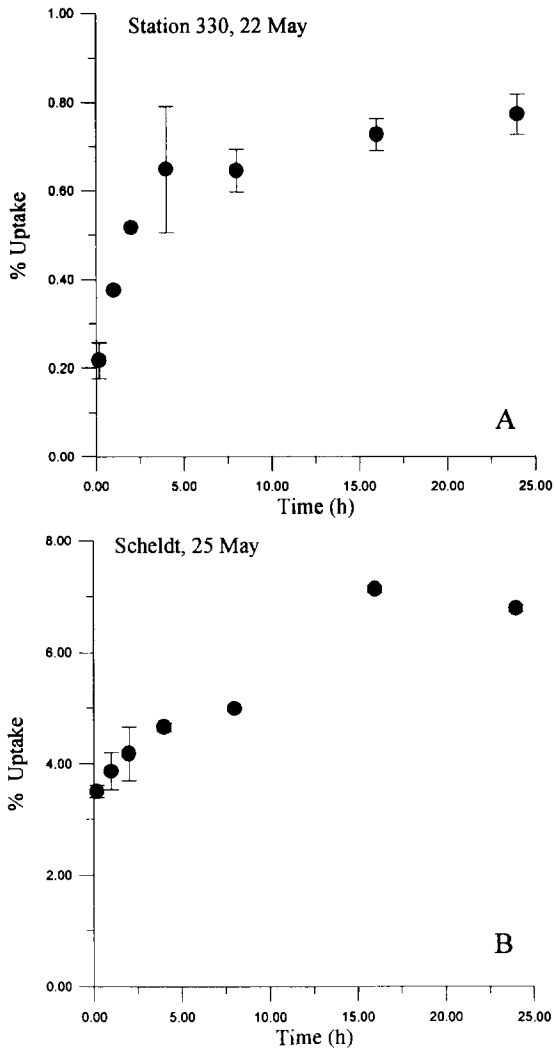

Fig. 1. Kinetics of ^{63}Ni uptake in samples from station 330 and the Scheldt estuary. Samples were treated with azide and incubated for 24 h under constant light. Error bars are the mean SE of two replicates.

min. This first period was followed by a stage of slower but still comparatively fast uptake until ~5 h, at which point there was a notable reduction in the uptake rates for both samples. It appears that equilibrium partitioning was not achieved in either sample by 24 h. (Although the Scheldt sample exhibited a slight decrease in % ^{63}Ni uptake after 15 h, possibly indicating equilibrium, further time points would be necessary to confirm this trend.) The fact that both samples exhibited similar changes in uptake rate over time, despite the undoubtedly higher number of uptake sites in the Scheldt sample, indicates that the extent of partitioning was limited by the slow reaction kinetics of Ni (Morel and Hering 1993) rather than by saturation of available Ni uptake sites.

The shape of these adsorption curves is similar to what has been observed for other metals in similar experiments (e.g. Al, Moran and Moore 1992; Zn and Cd, Wollast and Loijens 1991), and so from this point of view the results are not surprising. Ni appears to interact with particles in much the same fashion as other divalent trace metal cations that have been studied, the only difference perhaps being slower reaction kinetics. This finding is consistent with complexation theory, which predicts slow complexation kinetics for Ni due to its low rate constant for water exchange (Morel and Hering 1993). The more interesting aspect of these results is the observed interplay between the various factors of salinity, particle concentration, and Ni reaction kinetics, as discussed above. Further speculation is beyond the limited scope of these data.

To evaluate further the parameters affecting ^{63}Ni uptake, we characterized three samples from station 330 with respect to their primary productivity (as determined by ^{14}C uptake) and suspended matter concentration. Figure 2 presents these results compared with the ^{63}Ni uptake in each sample (24 h, light incubation). On the basis of replicate analyses, these differences in ^{63}Ni uptake are significant. It is apparent that the sample of 22 May had the highest ^{63}Ni uptake, despite the fact that it had the lowest suspended matter concentration of the three samples. The sample of 5 June had almost twice the ^{63}Ni uptake of the sample of 15 May ($0.26\pm0.01\%$ as opposed to $0.14\pm0.01\%$), although the suspended matter concentration of both samples was about the same. This result suggests that the quality of the suspended matter, rather than its quantity, was a determining factor in the scavenging capacity of these samples.

A further possibility is that ^{63}Ni uptake was affected by some biologically driven process that was independent of suspended matter concentration. Active uptake by phytoplankton, for example, could explain why there was a weak correlation between ^{14}C and ^{63}Ni up-

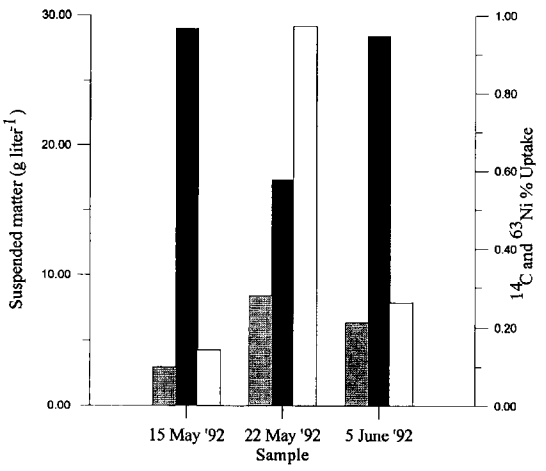

Fig. 2. Correlation of suspended matter concentration and ^{14}C uptake with ^{63}Ni uptake for three station 330 samples. Black bars represent suspended matter concentration, shaded and open bars represent ^{14}C and ^{63}Ni uptake, respectively. ^{63}Ni uptake was determined after incubation under constant light for 24 h, followed by filtration through a 0.45-μm cellulose acetate filter. ^{14}C uptake was also determined after 24 h of incubation.

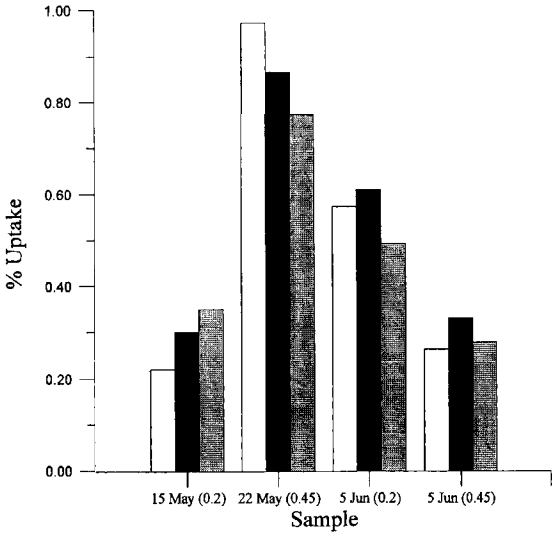

Fig. 3. Comparison of ^{63}Ni uptake in station 330 samples at 24 h under different incubation conditions. Open bars represent light incubations, black and shaded bars represent dark and azide incubations, respectively. Pore size of the filters used to collect particles (0.2 or 0.45 μm) is indicated in parentheses next to the sample date. Values shown are the mean of two replicates. Mean standard errors for these values are on the order of 5–8%.

take in these samples (Fig. 2). Because this data set was too small to permit a statistically significant analysis of such patterns, controlled experimentation was necessary to evaluate the effect of biological activity.

In Fig. 3, ^{63}Ni uptake results for the same three samples under different incubation conditions are compared. No significant trends are observable in the response of ^{63}Ni uptake to different levels of biological activity during 24 h of incubation, suggesting that this was not the major determining factor in ^{63}Ni uptake on this time scale. Differences in the partitioning of ^{63}Ni in these three samples are then apparently related to differences in their particulate composition. (The influence of dissolved substances is beyond the scope of this experiment.) It should be noted that, due to the elevated levels of Ni added to these samples as a consequence of using noncarrier-free ^{63}Ni, some biologically mediated uptake pathways of significance in natural systems may have been saturated. Therefore these results do not necessarily reflect primary uptake mechanisms operative in natural waters.

In an attempt to examine further the particle-specificity of ^{63}Ni uptake in these samples, some rudimentary size fractionation with 0.2- and 0.45-μm cellulose ester filters was attempted in the 5 June sample. These results are also shown in Fig. 3. The 0.2-μm filters were substantially more efficient at retaining particulate ^{63}Ni, indicating that a quantitatively significant fraction of the tracer was incorporated into particles <0.45 μm in size, such as bacteria or colloids. This effect is most likely due to the high ratio of surface area to volume of such particles. Similar results have been noted in other size-fractionation studies of oceanic particulate material (e.g. Moran and Buesseler 1992).

The picture of Ni partitioning that emerges thus far from this limited set of liquid scintillation data is controlled by abiotic sorption processes and limited by slow reaction kinetics. While the effect of particle concentration seemed to dominate in the extreme environment of the Scheldt estuary, in the station 330 samples there appeared to be some particle-specific effect in operation, possibly related to ratios of particle surface area to volume. We next discuss how qualitative autoradiographic data complemented this information.

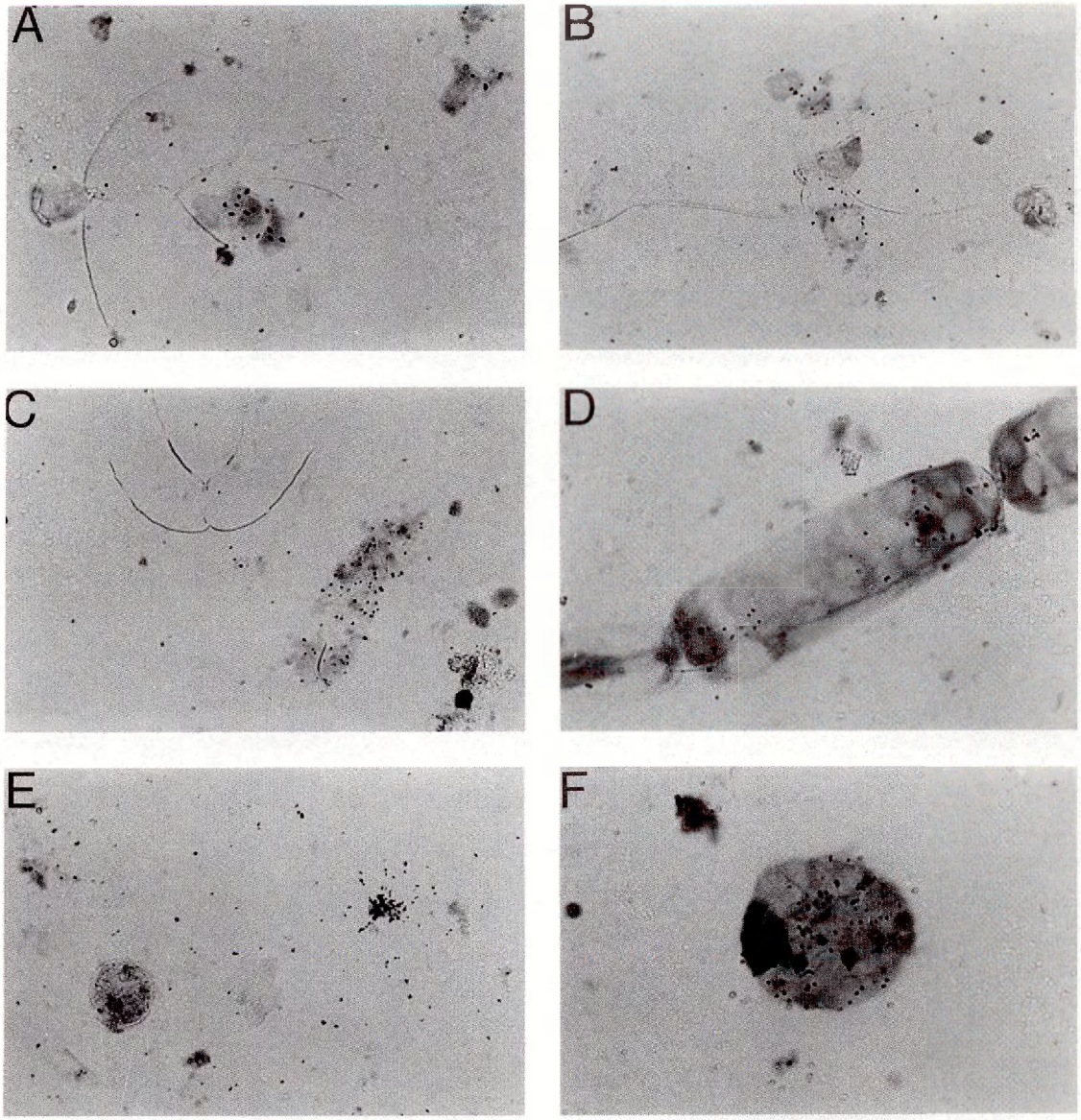

Fig. 4. Autoradiograms made from station 330 sample, 19 March. A–C. *Chaetoceros*. D–F. Other planktonic organisms. All microphotographs shown at 125× magnification except panel F, which is at 400×.

In Figs. 4 and 5, examples of autoradiograms (transmitted light, methyl-green pyronin stain) are shown. Epiflourescent microscopy was also applied in this investigation, but facilities to photograph slides under epifluorescent light were not available. The intent of these figures is to show that autoradiography of trace-metal sorption is possible and to give some indication of the quality of visual information obtainable through use of the technique as described here.

The autoradiograms in Fig. 4 were made from a station 330 sample taken on 19 March. Fig. 4A–C depicts labeled and unlabeled *Chaetoceros* cells. It is evident that even closely associated organisms displayed considerable variation in their degree of ^{63}Ni uptake (Fig. 4A, B) and that cells located adjacent to labeled

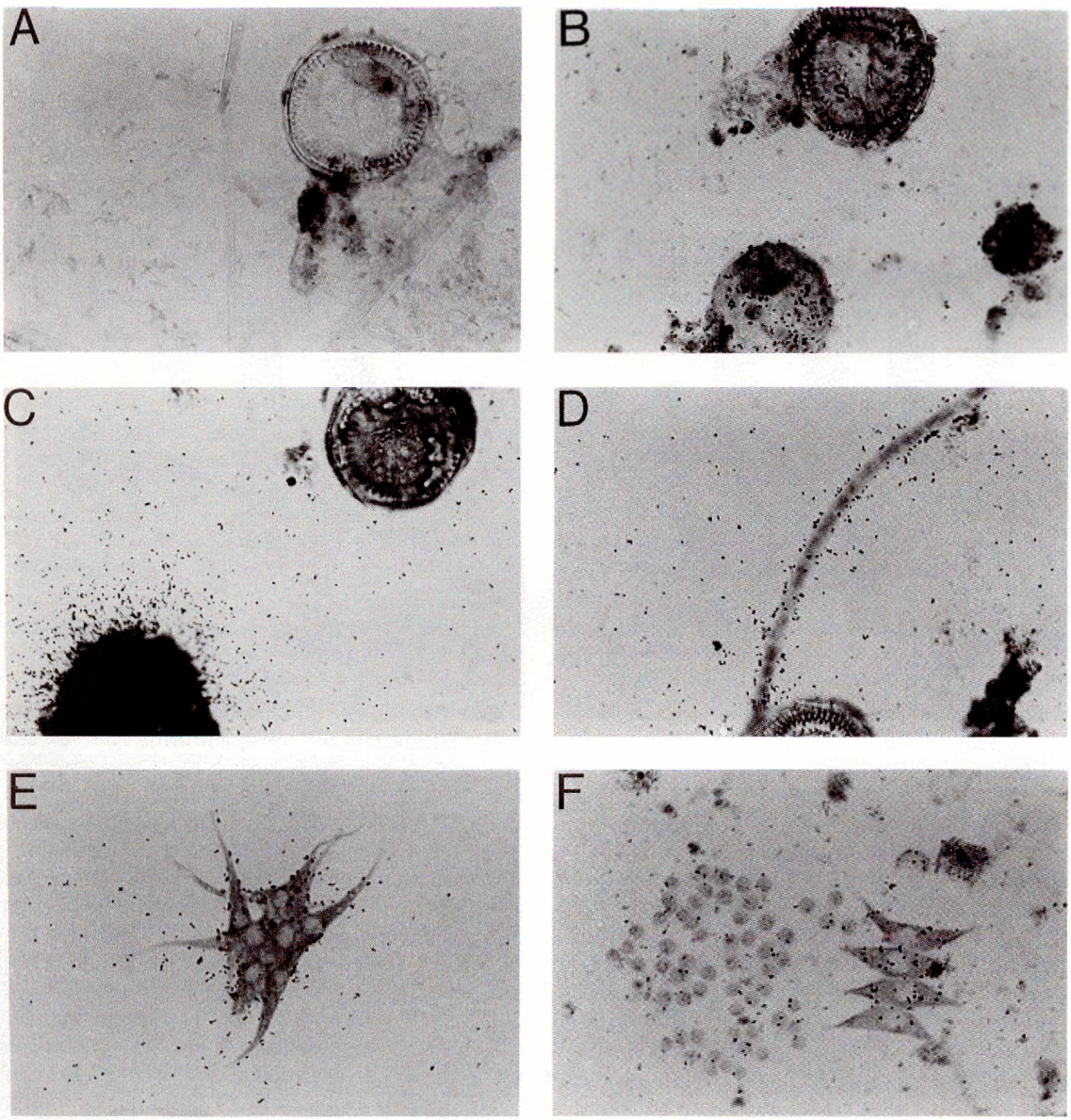

Fig. 5. Autoradiograms made from the Scheldt sample. A. An unlabeled control. B–D. The dominant diatom of the sample in close proximity to labeled objects. E, F. Labeled *Scenedesmus*- and *Microcystis*-type organisms. All microphotographs shown at 125× magnification except panel E, which is at 400×.

detritus were not necessarily labeled themselves (Fig. 4C). Figure 4D shows a filamentous alga with labeling at either end of the cell. In Fig. 4E, a diatom (unlabeled) is shown in close proximity to a highly labeled, unidentified object. Figure 4F shows an unidentified labeled alga, most likely a dinoflagellate. The grains that appear to be isolated in several photos (Fig. 4E, especially) are most probably due to small particles (<1.0 μm) that are obscured by the silver grains themselves in transmitted light. Examination of DAPI-stained autoradiograms of this sample revealed labeling of free bacteria and other cells of bacterial size. Most of the labeling in the sample was distributed between the small particle size frac-

tion and detrital particles. Background in controls for the 19 March sample set was somewhat higher than for later station 330 samples—on the order of 10 grains per oil-immersion field.

The Scheldt estuary sample, collected on 25 May, represented a very different water mass from that sampled at station 330. Despite the much greater complexity of its particle matrix, however, the autoradiographic method was equally applicable. Examples of autoradiographic data obtained from the Scheldt sample (methyl-green pyronin stain, transmitted light) are shown in Fig. 5. (Fig. 5A is a photograph of an unlabeled control slide, displaying the extremely low background obtained with this technique.) The large diatom visible in Fig. 5B and C was the dominant phytoplankton in the sample. The diatom is unlabeled in these photographs, despite the close proximity of a labeled dinoflagellate-type cell (Fig. 5B) and a highly labeled, possibly inorganic, particle (Fig. 5C). The dominant diatom species was not associated with silver grains in any of the autoradiograms examined.

In Fig. 5D–F, other types of phytoplankton (forms similar to *Oscillatoria, Scenedesmus,* and *Microcystis*) are shown with associated silver grains. These species exhibited variable labeling in overall autoradiographic analysis. DAPI-stained autoradiograms of the Scheldt sample revealed high densities (generally >50 per field) of labeled free-living bacteria and similarly sized particles. The presence of such labeled objects may account for the high numbers of apparently isolated grains in Fig. 5B–F, in which the small particles could be obscured by the silver grains in transmitted light, as explained for the station 330 sample in Fig. 5E.

Considering the high productivity of this estuarine environment, another possible explanation for these grains is that they are associated with bioproduced unorganized extracellular polymeric material (i.e. "slime") which was not stained by the DNA-specific stains used in this study. DAPI autoradiograms revealed that whole algal cells were generally free of bacteria, so the labeling of phytoplankton in these photographs can be primarily attributed to their own ^{63}Ni adsorption. Detrital and inorganic particles exhibited a variable labeling pattern overall, with some particles apparently adsorbing large amounts of ^{63}Ni (*see Fig. 5C*).

Table 2 summarizes the particulate speciation and autoradiographic labeling patterns for all samples. It can be seen that where bacteria and small cells were present, free-living forms were consistently labeled. Small detrital particles were also consistently associated with developed grains. This finding supported the liquid scintillation data, which indicated that ^{63}Ni sorption by particles <0.45 μm was quantitatively significant.

The significance of ^{63}Ni labeling on larger detrital material varied from sample to sample. In some cases (station 330, 19 March) detritus appeared to account for much of the labeling, while in others (station 330, 22 May) phytoplankton cells dominated ^{63}Ni uptake. In the 22 May sample from station 330, the dominant phytoplankton (a form similar to *Ankistrodesmus*) was shown to be consistently associated with the tracer, while *Phaeocystis* did not appear to sorb ^{63}Ni in any slide examined. The large amounts of senescent *Phaeocystis* in the 15 May sample from station 330 did not appear to be labeled either. (It should be noted that the large size of *Phaeocystis* colonies made autoradiographic analysis difficult because of uneven emulsion coating and chemographic desensitization in some cases. It is possible that *Phaeocystis* may have sorbed more ^{63}Ni than was indicated by autoradiographic analysis, although liquid scintillation results were not contradictory.) The presence of a phytoplankter with a high affinity for ^{63}Ni may explain why the 22 May sample exhibited significantly greater ^{63}Ni uptake than samples taken on 15 May and 5 June, despite its somewhat lower suspended solid load (Fig. 2).

The autoradiographic data on the station 330 sample of 22 May serves to demonstrate the utility of autoradiographic techniques for determining the distribution of label over objects within the same general size class. In the Scheldt sample, for another example, the dominant centric diatom was shown to be entirely nonassociated with ^{63}Ni, while other large phytoplankton in the sample displayed various degrees of labeling. In such a complex matrix, this information would be impossible to obtain by conventional filter-and-count methods because size fractionation with filters would be too inaccurate.

The use of autoradiography modified and contributed to the view of ^{63}Ni partitioning obtained by liquid scintillation data in several

Table 2. Summary of autoradiographic analysis of station 330 and Scheldt samples. "Large cells" (>2 μm) includes those forms analyzed on methyl-green pyronin-stained autoradiograms. "Small cells" (<1 μm) designates forms analyzed on DAPI-stained autoradiograms. Detrital and inorganic material was analyzed with both types of stains, depending on the same size range.

Sample	Particulate fractions	Ni uptake patterns
Station 330, 19 March (*see Fig. 4*)	Large cells—*Chaetoceros* dominant, also a few colonies of *Phaeocystis* and unidentified diatoms, dinoflagellates, and filamentous algae	Large cells—*Chaetoceros* rarely labeled, *Phaeocystis* never; other species too few to generalize
	Small cells—free-living bacteria	Small cells—consistently labeled
	Detritus—dense aggregates in 5-μm size range	Detritus—labeling highly variable, but generally more significant than cellular labeling
Scheldt, 25 May (*see Fig. 5*)	Large cells—centric diatom dominant, also forms similar to *Scenedesmus, Microcystis,* and *Oscillatoria* present	Large cells—no labeling of centric diatom, variable labeling of other species
	Small cells—high densities (>50 per field) of free bacteria, rods dominant; also bacteria associated with detritus	Small cells—consistently labeled when in free state
	Detritus—large amounts in all size ranges, some large plant fragments	Detritus—smaller pieces consistently labeled, larger ones variable
	Inorganics—frequent occurrence of mineral particles	Inorganics—inconsistent, at times intensely labeled
Station 330, 15 May	Large cells—very few intact *Phaeocystis* colonies, some ciliates	Large cells—nonlabeled
	Small cells—free-living bacteria, some attached to detritus	Small cells—consistent labeling of free-living forms
	Detritus—large amount of senescent *Phaeocystis*	Detritus—nonlabeled
Station 330, 22 May	Large cells—*Ankistrodesmus*-type dominant, few *Phaeocystis*	Large cells—*Ankistrodesmus*-type consistently labeled, *Phaeocystis* not labeled
	Small cells—very few (<10 per field)	Small cells—too few to generalize
	Detritus—small amount of larger, relatively dense aggregates (5–10 μm)	Detritus—variable labeling, insignificant relative to large cells
Station 330, 5 June	Large cells—very few unidentified diatoms and coccoliths	Large cells—too few to generalize
	Small cells—free-living coccoid bacteria, small phytoplankton	Small cells—consistently labeled
	Detritus—large amounts of thin, filmy material and smaller (<5 μm) dense aggregates	Detritus—less dense material not labeled, aggregates variably labeled

ways. In the most general sense, the importance of small (<1.0 μm) particles as sorption sites was confirmed by comparing tracer distribution between small and large objects. More significantly, autoradiography demonstrated that particle-specific effects were operative on objects in the algal size range. This finding has important implications for scavenging studies, since it is particles in the larger size class that are responsible for the downward flux of scavenged material.

In this experiment both liquid scintillation and microautoradiographic methods were applied to the study of ^{63}Ni partitioning in natural water samples. Results indicate that Ni sorption under the conditions described here was a primarily abiotic, passive chemisorption process. Partitioning was limited in extent on a 24-h time scale by the slow reaction kinetics of Ni. While small particles were shown to be quantitatively significant sorption sites, sorption behavior of the larger-sized particle pool was shown to be patchy and, in some cases, highly particle-specific.

This work has demonstrated that microautoradiography can be successfully applied to

the study of trace metal–particle interactions. The potential of the method is clear, even though it has been used here only in the most qualitative capacity. Although autoradiography will never be as quantitative in the absolute sense as other, detection-based methods of counting radioactivity, relative quantitation is possible when the proper controls and statistical counting methods are applied (e.g. Brock and Brock 1968). Sensitivity could also be markedly improved by using a carrier-free tracer. Thus, although 60 nM was the concentration of noncarrier-free tracer necessary to achieve our results, lower tracer levels (7–8 nM) are certainly possible.

Although the utility of autoradiography may currently be most apparent when dealing with highly complex, heterogeneous systems where filter fractionation is inefficient, wider applications can be considered. Selective stains, for example conjugated lectins for isolating carbohydrate moities (Cushion et al. 1988), could be combined with microautoradiography to study the role of particle surface chemistry in trace-metal scavenging. Eventually, further refinement of the method could permit its use at the level of electron microscopy for the localization of specific metal receptor sites on cell surfaces and within cells. Additional metal isotopes to which this technique could possibly be applicable include ^{51}Cr, ^{55}Fe, ^{65}Zn, ^{109}Cd, ^{139}Ce, ^{203}Hg, ^{210}Pb, and ^{234}Th. Further research is needed to determine whether suitable parameters can be established for high efficiency, high resolution microautoradiography of these isotopes.

Katherine Barbeau[1]
Roland Wollast

Laboratory of Chemical Oceanography
Free University of Brussels
Campus Plaine, C.P. 208., Bd. du Triomphe
1050 Brussels, Belgium

References

BROCK, M. L., AND T. D. BROCK. 1968. The application of micro-autoradiographic techniques to ecological studies. Mitt. Int. Ver. Theor. Angew. Limnol. 15, p. 1–29.

BRULAND, K. W. 1980. Oceanographic distributions of cadmium, zinc, nickel, and copper in the North Pacific. Earth Planet. Sci. Lett. **49:** 45–56.

CUSHION, M. P., J. A. DESTEFANO, AND P. D. WALZER. 1988. *Pneumocystis carinii*: Surface reactive carbohydrates detected by lectin probes. Exp. Parasitol. **67:** 137–147.

DAVENPORT, J. B., AND B. MAGUIRE, JR. 1984. Quantitative grain density autoradiography and the intraspecific distribution of primary productivity in phytoplankton. Limnol. Oceanogr. **29:** 410–416.

DOUGLAS, D. J., J. A. NOVITSKY, AND R. O. FOURNIER. 1987. Microautoradiography-based enumeration of bacteria with estimates of thymidine-specific growth and production rates. Mar. Ecol. Prog. Ser. **36:** 91–99.

DURIE, B. G., AND S. E. SALMON. 1975. High speed scintillation autoradiography. Science **190:** 1093–1095.

FOWLER, S. W., L. F. SMALL, AND J. M. DEAN. 1970. Distribution of ingested zinc-65 in the tissues of some marine crustaceans. J. Fish. Res. Bd. Can. **27:** 1051–1058.

HONEYMAN, B. D., AND P. H. SANTSCHI. 1988. Critical review: Metals in aquatic systems. Environ. Sci. Technol. **22:** 862–871.

HUTCHINS, D. A., G. R. DITULLIO, AND K. W. BRULAND. 1993. Iron and regenerated production—evidence for biological iron recycling in two different marine environments. Limnol. Oceanogr. **38:** 1242–1255.

JANNASCH, H. W., B. D. HONEYMAN, L. S. BALISTRIERI, AND J. W. MURRAY. 1988. Kinetics of trace element uptake by marine particles. Geochim. Cosmochim. Acta **52:** 567–577.

KNOECHEL, R., AND J. KALFF. 1976. The applicability of grain density autoradiography to the quantitative determination of algal species production: A critique. Limnol. Oceanogr. **21:** 583–589.

LANCELOT, C., AND S. MATHOT. 1987. Dynamics of a *Phaeocystis*-dominated spring bloom in Belgian coastal waters. 1. Phytoplanktonic activities and related parameters. Mar. Ecol. Prog. Ser. **37:** 239–248.

MEYER-REIL, L.-A. 1978. Autoradiography and epifluorescence microscopy combined for the determination of number and spectrum of actively metabolizing bacteria in natural waters. Appl. Environ. Microbiol. **36:** 506–512.

MOFFETT, J. W. 1990. Microbially mediated cerium oxidation in sea water. Nature **345:** 421–423.

MORAN, S. B., AND K. O. BUESSELER. 1992. Short residence time of colloids in the upper ocean estimated from $^{234}Th/^{238}U$ disequilibria. Nature **359:** 221–223.

———, AND R. M. MOORE. 1992. Kinetics of the removal of dissolved aluminum by diatoms in seawater: A comparison with thorium. Geochim. Cosmochim. Acta **56:** 3365–3374.

MOREL, F. M. M., AND J. G. HERING. 1993. Principles and applications of aquatic chemistry. Wiley.

NYFFELER, U. P., Y.-H. LI, AND P. H. SANTSCHI. 1984. A kinetic approach to describe trace-element distribution between particles and solution in natural aquatic systems. Geochim. Cosmochim. Acta **48:** 1513–1522.

PORTER, K. G., AND Y. S. FEIG. 1980. The use of DAPI for identifying and counting aquatic microflora. Limnol. Oceanogr. **25:** 943–948.

[1] Present address: Department of Marine Chemistry and Geochemistry, Woods Hole Oceanographic Institution, Woods Hole, Massachusetts 02543

ROGERS, A. W. 1973. Techniques of autoradiography. Elsevier.

TABOR, P. S., AND R. A. NEIHOF. 1982. Improved microautoradiographic method to determine individual microorganisms active in substrate uptake in natural waters. Appl. Environ. Microbiol. **44**: 945–953.

WARD, B. B. 1984. Combined autoradiography and immunofluorescence for estimation of single cell activity by ammonium-oxidizing bacteria. Limnol. Oceanogr. **29**: 402–409.

WOLLAST, R., AND M. LOIJENS. 1991. Study of the scavenging of trace metals in marine systems using radionuclides, p. 154–163. *In* Radionuclides in the study of marine processes—Radstomp '91. Symp. Proc.

Submitted: 2 February 1993
Accepted: 20 December 1993
Amended: 8 February 1994

Limnol. Oceanogr., 39(5), 1994, 1222–1227

Disequilibrium between ^{226}Ra and supported ^{210}Pb in a sediment core from a shallow Florida lake

Abstract—^{210}Pb dating can be used to assign ages in lake sediment cores, calculate rates of sediment accumulation, and determine the timing of recent changes in lake-watershed ecosystems. We used low-background gamma counting to measure ^{226}Ra and total ^{210}Pb activities in a core from Lake Rowell, Florida. ^{226}Ra activity was high and strongly variable throughout the core, even exceeding total ^{210}Pb activity in recently deposited sediments. We traced one source of Ra-rich sediments to the only inflow, Alligator Creek, where stream-bottom deposits display disequilibrium between ^{226}Ra and supported ^{210}Pb. High and variable ^{226}Ra activity in the Lake Rowell profile argues for direct estimates of in situ Ra in lake sediment cores from disturbed watersheds that have Ra-bearing bedrock. Isotopic disequilibrium between ^{226}Ra and supported ^{210}Pb makes it difficult to distinguish between supported and unsupported ^{210}Pb activity throughout the Lake Rowell core and would require special assumptions and nonconventional dating models to establish age-depth relationships.

^{210}Pb dating is used widely to determine the age of recent lake sediments. The dating method is invaluable for establishing the timing of ecological changes, especially in lakes for which long-term limnological data are lacking. The procedure yields a sediment age-depth relationship that extends back in time 100–150 yr.

Acknowledgments

Thomas Whitmore assisted with sample collection. Emmett Bolch, Michael W. Binford, and David Hodell provided discussions. We thank John Robbins and two anonymous reviewers for comments.

^{210}Pb is a naturally occurring radionuclide that has a half-life of 22.3 yr. Core dating requires estimation of unsupported ^{210}Pb activity in a sediment section (often called atmospherically derived, excess or fallout ^{210}Pb activity) and application of an appropriate dating model (Appleby and Oldfield 1978; Robbins and Herche 1993).

The ultimate source of unsupported ^{210}Pb in lake sediments is radioactive decay of ^{226}Ra in local rocks and soils. ^{226}Ra decays to radon (^{222}Rn) that outgases to the atmosphere. Rn gas ($t_{1/2}$ = 3.8 d) decays rapidly through several short-lived daughters (^{218}Po–^{214}Pb–^{214}Bi–^{214}Po) to ^{210}Pb that is ultimately deposited on land and lake surfaces (El-Daoushy 1988). Some of the ^{210}Pb that reaches a lake is adsorbed to fine particles and incorporated into accumulating sediments. ^{210}Pb is also produced via the decay of in situ ^{226}Ra that is part of the sediment matrix. ^{210}Pb derived from this source is called supported ^{210}Pb.

^{210}Pb activity in lake sediments can be assessed by alpha or gamma detection. Alpha counting involves the measurement of the granddaughter nuclide ^{210}Po and assumes ^{210}Po/^{210}Pb equilibrium (Joshi 1989), whereas gamma counting measures ^{210}Pb decays directly (Appleby et al. 1986). Supported ^{210}Pb activity is often estimated by the mean of several low-activity, downcore samples. Supported ^{210}Pb activity is assumed to be constant throughout the profile, and unsupported activ-